Received: 15 May 2018 | Revised: 3 November 2018 | Accepted: 15 November 2018
DOI: 10.1002/gj.3416

RESEARCH ARTICLE

WILEY

The basement and volcanic activities of the Xisha Islands: Evidence from the kilometre-scale drilling in the northwestern South China Sea

Yu Zhang[1,2,3] | Kefu Yu[1,2,3] | Handong Qian[4] | Tianlai Fan[1,2,3] | Yuanfu Yue[1,2,3] | Rui Wang[1,2,3] | Wei Jiang[1,2,3] | Shendong Xu[1,2,3] | Yinghui Wang[1,2,3]

[1] Guangxi Laboratory on the Study of Coral Reefs in the South China Sea, Guangxi University, Nanning, China

[2] Coral Reef Research Center of China, Guangxi University, Nanning, China

[3] School of Marine Sciences, Guangxi University, Nanning, China

[4] School of Earth Sciences and Engineering, Nanjing University, Nanjing, China

Correspondence
Kefu Yu, School of Marine Sciences, Guangxi University, Nanning 530004, China.
Email: kefuyu@scsio.ac.cn

Funding information
Natural Science Foundation of China, Grant/Award Number: 91428203; Guangxi University, Grant/Award Number: XBZ170339; Education Department of Guangxi Zhuang Autonomous Region, Grant/Award Number: 2018KY0045; Science and Technology Department of Guangxi Zhuang Autonomous Region, Grant/Award Numbers: AD17129063 and AA17204074

Handling Editor: S. Li

As one of the microcontinents dispersed in the South China Sea (SCS), the Xisha microcontinent lacks the petrological evidence of the Cenozoic magmatic activity and basement. Well CK-2, as a full-coring kilometre-scale major scientific drilling in Xisha Islands in the northwestern SCS, drilled through the thick reefal limestone and into the underlying basaltic pyroclastic rocks basement. This paper presents zircon U–Pb age and mineral chemistry of clinopyroxenes from the basaltic pyroclastic rocks. Mineral composition of the clinopyroxenes suggests that most of the clinopyroxenes are composed of diopside, which contains relatively high Al(*w* (Al_2O_3) = 5.03%–10.25%) and Ti(*w* (TiO_2) = 2.2%–4.95%). The clinopyroxene discrimination diagrams show that the primary magma is alkaline basalt and likely generated in an intraplate tectonic setting. U–Pb dating of zircons by LA-ICP-MS yielded a wide range of ages: 36–33, 116–104, 148–140, 207–196, 255–236, 440, 808–749, and 2,440–1185 Ma. The youngest group has an average age of 35.5 ± 0.9 Ma, which is considered as the maximum age of the basalt eruption. The 2440 ± 19 Ma, which is the oldest zircons in the SCS, are firstly found in the basaltic pyroclastic rocks from the SCS, suggesting that the SCS may contain very old materials. The ages of the inherited zircons are comparable to magmatic activities that occurred around the SCS, implying that they were probably once linked and an integrated part of Gondwana. The ancient continental basement has experienced multistages magmatic events.

KEYWORDS
basaltic, clinopyroxene, South China Sea, zircon

1 | INTRODUCTION

The South China Sea (SCS) is located in the junction of the Eurasian Plate, the Pacific Plate, and the Indian–Australian Plate (Figure 1). It is a typical representative of western Pacific marginal seas (Li, Li, Yu, Wang, & Jourdan, 2015; Lei et al., 2016; Liu et al., 2016; Lü, Hao, Yao, Xing, & Qiu, 2016; Guo et al., 2016; Zhu, Li, Sun, & Li, 2016; Zhang, Li, Guo et al., 2016; Zheng et al., 2016). Despite its relatively short tectonic evolution history, the SCS has roughly experienced a complete Wilson cycle, including continental break-up, seafloor spreading, and subduction (Fang, Ding, Fang, Zhao, & Feng, 2016; Li, Yan, Chen, & Shi, 2013; Wang et al., 2016; Yang & Fang, 2015). Therefore, the SCS was regarded as an excellent natural laboratory for studying continental break-up, sedimentary basin formation, mantle and lithosphere evolution, and land–ocean interactions (Franke, 2013; Hsieh, Shellnutt, & Yeh, 2016; Li et al., 2013; Li, Li, Yu, et al., 2015; Taylor & Hayers, 1983; Yan, Shi, Liu, Wang, & Bu, 2010; Yan, Shi, Yang, & Wang, 2008).

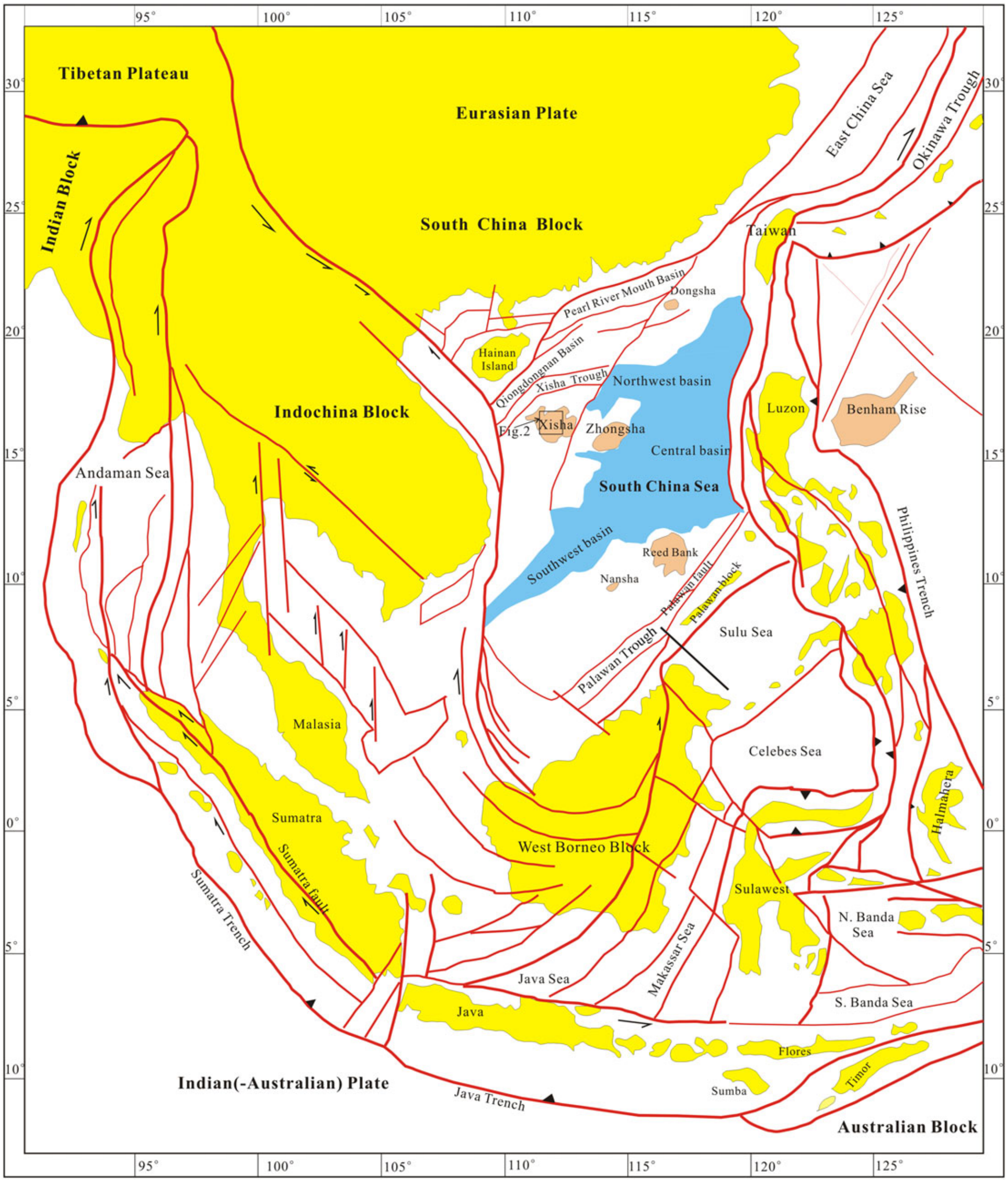

FIGURE 1 Tectonic sketch map of the SCS and its surround area (modified from Xu, Avraham, Kelty, & Yu, 2014) [Colour figure can be viewed at wileyonlinelibrary.com]

The basement is the material basis for the evolution of the basin and is closely related to ocean evolution. The basement research is an important part of the study of tectonic evolution of the basin. Because the thick sediments in the SCS, there are few basement rocks dispersed in the SCS, which led to the lack of the research on the nature of the basement rocks. Qin (1987) reported the discovery of gneissic granite from the basement of Well XY-1. Based on the Rb–Sr and K–Ar ages of the gneissic granite from Well XY-1, Sun (1987) suggested that the Xisha basement was probably formed in the Palaeozoic. The zircon U–Pb ages for granitic from the Nanshan microblocks indicates that there exists Precambrian crystalline basement within microblocks in the SCS (Yan, Shi, Wang, & Liu, 2008; Yan et al., 2010). The basement of Well XK-1 consists of amphibole plagiogneisses (152.9 ± 1.7 Ma) and the early granitic rocks (107.8 ± 3.6 Ma; Zhu et al., 2017). In addition, Lu et al. (2011) identified the Precambrian crystalline basement based on the geophysical data in the northern margin of the SCS.

Volcanic rocks could be used as a probe for deep processes and magmatic activities. The volcanic continental margins were genetically associated with mantle plumes. In contrast, nonvolcanic rifted margins, where the lithosphere was extensively, are characterized by weak volcanism (Yan, Deng, Liu, Zhang, & Jiang, 2006). The Cenozoic magmatic activities in the SCS and its surroundings are generally considered to be related to the expansion of the SCS (Huang, Niu, Xu, Ma, & Qiu, 2013; Hui, Li, Li, Guo et al., 2016; Xu, Wei, Qiu, Zhang, & Huang, 2012). The investigation of IODP 349 suggests that the opening of the SCS started at 33 Ma and ended at 15 Ma (Ding & Li, 2016; Li, Li, Ding et al., 2015; Li, Li, Yu, et al., 2015). As one of the biggest marginal seas in the West Pacific, Cenozoic volcanism in the SCS and its surrounding areas are divided into three groups: prespreading, syn-spreading, and postspreading, based on the relationship with the expansion of the SCS-spreading events (Hui, Li, Li, Guo, et al., 2016; Xie, Zhong, & Yan, 2017; Xu et al., 2012). However, due to the thick sediments on the seafloor in the SCS, it is difficult to gain the volcanic rocks from the SCS. Thus, only a few researches on the Cenozoic volcanic rocks have been done in the SCS, which seriously constrains us to understand the Cenozoic basaltic volcanism of the SCS. During performing national investigation program for coral reef, we performed a kilometre-scale deep drill (Well CK-2; 110°0′53.557″E, 16°26′56.368″N) in Chenhang Island of Xisha Islands, SCS, and obtained about 50-m basaltic pyroclastic rocks, which are the first obtained basaltic rock basement in Xisha Islands. In this study, based on the petrographic investigation, we present the new observations as well as zircon U–Pb dating and mineral chemistry of clinopyroxene of basaltic pyroclastic rocks in order to better constrain the basement and volcanic activity in the SCS.

2 | GEOLOGICAL SETTING AND SAMPLE DESCRIPTION

Tectonically, the SCS can be subdivided into three parts: the northern continental margin, the southern continental margin, and the ocean basin. According to the water depth and submarine topography features, the SCS basin can be divided into three subbasins: the northwest basin, the central subbasin, and the southwest basin (Figure 1; Li, Li, Yu, et al., 2015; Zhang, Li, Ruan et al., 2016). The main geological features of the SCS include East Vietnam Fault in the west, the Palawan Trench in the south, the Manila Trench in the east, and the northern transition zone (Hui, Li, Li, Zhang et al., 2016; Xu et al., 2016; Yan, Shi, Wang, Bu, et al., 2008). The northern margin is located between the South China Block and the SCS continent–ocean transition zone. It is composed of a series of Cenozoic extension basins. The eastern margin is a subduction zone. The southern margin is mainly a compressive collision zone. The southern margin is a strike-slip pull-apart zone, and a series of oil and gas basins are developed (Shi & Yan, 2011; Wan et al., 2006; Yan, Shi, Yang, et al., 2008; Yan, Shi, Wang, Bu, et al., 2008). In addition, there are several microcontinents dispersed in the SCS, including Xisha-Zhongsha Block, Nansha Block, and Reed-Northeastern Palawan Block (Li et al., 2018; Yan et al., 2015; Yan, Shi, Wang, et al., 2008; Yan, Shi, Yang, et al., 2008; Yao, Wan, & Wu, 2004). These microcontinents were regarded as an integrated block during Paleo-Tethys times, which was named “Qiongdongnan block” (Liu et al., 2004; Liu, Yan, Liu, & Deng, 2006). The basement of the SCS is mainly composed of the Precambrian metamorphic crystalline basement and experienced the Yanshanian tectonic magma event (Yan et al., 2015; Yan, Shi, Wang, et al., 2008). After the expansion of the SCS, there have been significant intraplate volcanisms in the SCS and surrounding areas. As a result, multiple sea mountains formed in the ocean basin, and there was immense alkaline basalt eruption in the surrounding areas of the SCS.

Xisha Islands are located in the continental slope of the northwestern SCS, with an area of 8 km^2 (Zhu et al., 2015). It is comprised of a series of islands, reefs, and shoals. The northern margin of the SCS is the Xisha Trough. The southern margin of the SCS is the deep-sea basin. The eastern margin of the SCS is the Zhongsha Trough. The western margin of the SCS is the SCS shelf. As far away from the mainland and appropriate conditions for coral growth, Xisha Islands deposited more than 1-km thick reef facies carbonate formation (Xiu et al., 2017). Well CK-2 is located in the Chenhang Island, Xisha Islands (Figure 2; 110°0′53.557″E, 16°26′56.368″N). It is a kilometre-scale major scientific drilling in Xisha Islands. The total length of the core is 928.75 m. The well drilled through the thick reefal limestone. It can be divided into two parts. From top to bottom: (a) carbonate rocks (0–878.21 m) and (b) basaltic volcanic clastic rocks (878.21–928.75 m; Figure 3). The basaltic pyroclastic rocks are conformable contact with overlying carbonate rocks. One representative basaltic pyroclastic rock sample (Zr1) was selected for zircon U–Pb dating. The location of sample Zr1 is shown in Figure 3. The basaltic pyroclastic rocks are grey green on fresh surfaces. The petrographic characteristics are vesicular structure and porphyritic texture. The phenocrysts are mainly composed of pyroxene, as well as amount of plagioclase. They are usually subangular or angular, suggesting the basaltic pyroclastic rocks are in situ or nearby volcanism. The groundmass consists of microcrystalline plagioclase, pyroxene, and basalt glass. Furthermore, there are a few marine fossils in the rocks (Figure 4). The pores in basaltic pyroclastic rocks are generally developed, with the geological characteristics of eruption of shallow sea. The basaltic pyroclastic rocks are weakly altered. The amygdales are round, oval-shaped, and irregular in shape, which was filled with carbonate calcite, zeolite, opal, and chalcedony.

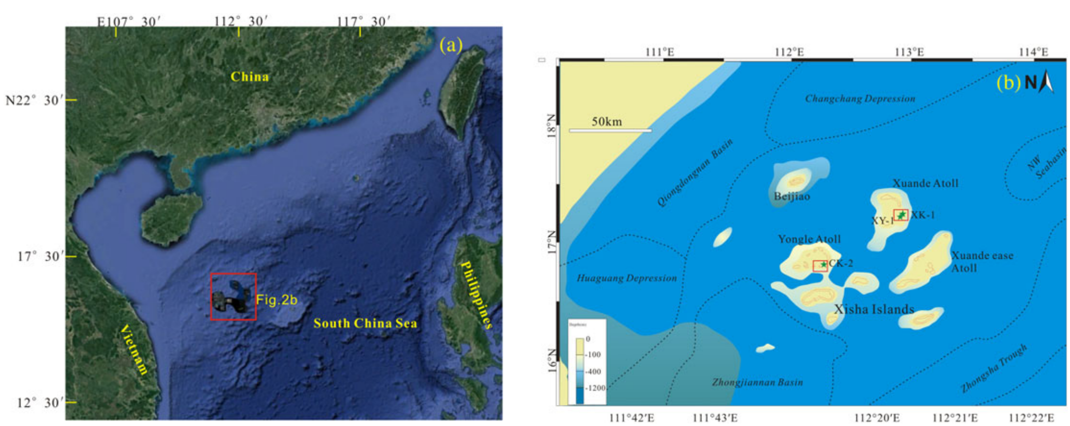

FIGURE 2 Study area and location of Well CK-2 (modified from Wang et al., 2018) [Colour figure can be viewed at wileyonlinelibrary.com]

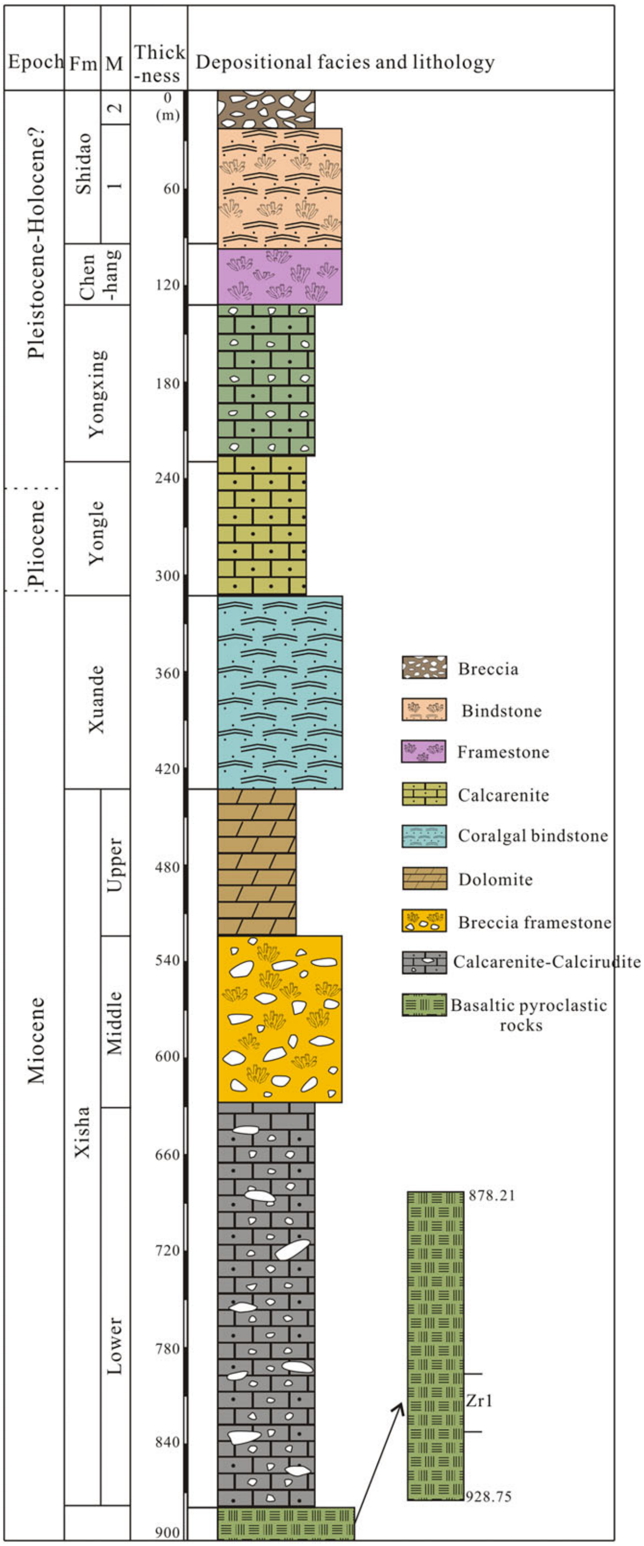

FIGURE 3 Stratigraphy of Well CK-2, Xisha Islands [Colour figure can be viewed at wileyonlinelibrary.com]

3 | ANALYTICAL METHODS

About 8-kg fresh sample was crushed in a corundum jaw crusher. The zircon grains were separated from the rock sample using conventional heavy liquid and magnetic techniques and then purified by hand picking under a binocular microscope. Then, zircons were mounted in epoxy blocks and polished to obtain an even surface. Cathodoluminescence (CL) images were taken at the Wuhan SampleSolution Analytical Technology Co., Ltd., Wuhan, China. Typical CL images were obtained to identify internal structures and choose potential target sites for U–Pb analyses. The guideline for choosing potential target sites is outlined in reference (Liu, Liu, Zhang, & Yang, 2011).

Zircon U–Pb dating was carried out using LA-ICP-MS at the School of Resources and Environmental Engineering, Hefei University of Technology. A pulsed 193-nm ArF Excimer (COMPex PRO) with laser power of 10-mJ/cm^2 pulse energy at a repetition ratio of 6 Hz coupled to an Agilent 7500a quadrupole ICP-MS was used for ablation. The diameter of the laser ablation crater was 32 μm. Zircon 91500 was used as an external standard for age calculation. NIST610 glass was used as an external standard for U, Th, and Pb concentration calculations. The detailed analytical procedure were similar to those describe by Yuan et al. (2008) and Zong et al. (2010). The isotopic data was processed using the ICPMS DataCa and ISOPLOT software (Liu et al., 2010; Ludwig, 2003). Common Pb corrections used the method proposed by Andersen (2002).

Mineral compositions in selected samples were analysed using a JXA 8100 electron microprobe at the Key Laboratory of Submarine Geosciences, Second Institute of Oceanography, State Oceanic Administration. The operating conditions were an accelerating voltage of 15 kV and beam current of 20 nA. A 5-μm beam diameter was used to analyse the clinopyroxene. Counting times were 10 s on peak and 10 s on background for all elements. Natural minerals and synthetic oxides were used as standards. Detection limits are typically 50–400 ppm. The precision for all analysed elements was <2.0%.

4 | RESULTS

4.1 | Mineral chemistry of clinopyroxene

The electron microprobe analyses results are shown in Table S1. The chemical composition of pyroxene in Well CK-2 was changed greatly, which showed the characteristics of high content in Al and Ti. The clinopyroxenes have 42.27% to 49.73% SiO_2, 2.2% to 4.95% TiO_2, 5.03% to 10.25% Al_2O_3, 6.35% to 8.02% FeO, 10.56% to 14.37% MgO, and 21.86% to 22.67% CaO. The Mg$^{\#}$ of the clinopyroxene is from 74.97 to 95.17.

According to Morimoto (1988) pyroxene classification and nomenclature, all the clinopyroxenes from Well CK-2 belonged to Ca–Mg–Fe series (Figure 5). On the Wo–En–Fs diagram (Figure 5), most of the clinopyroxenes fall in the field of diopside ($Wo_{45.77–49.89}En_{33.34–41.5}Fs_{10.36–14.25}$).

4.2 | Zircon U–Pb dating

U–Pb ages have been determined for 81 zircon grains from the basaltic pyroclastic rocks. The results of zircon dating are listed in Table S2. CL images of representative zircons from sample Zr1 are shown in Figure 6. Th/U ratios of zircons range from 0.25 to 1.77, consistent with a magmatic origin (Hoskin & Ireland, 2000; Hoskin & Schaltegger, 2003).

Zr1 has an available age number of 39 (concordance >90%). There was a large range in zircon U–Pb ages. The age population is grouped

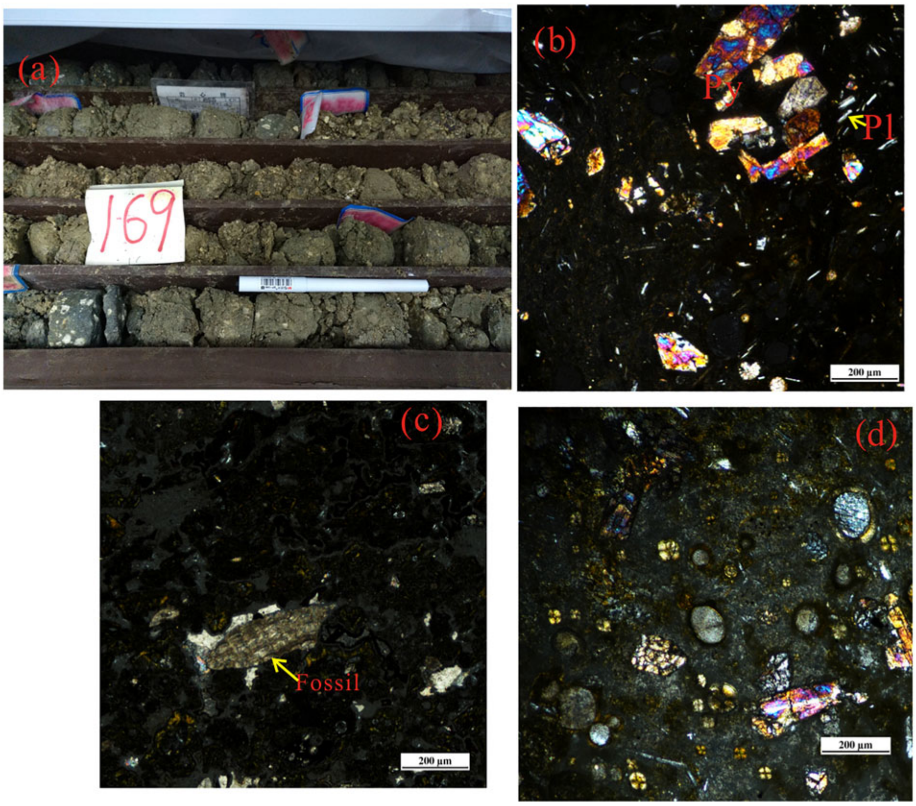

FIGURE 4 Photographs of the basaltic pyroclastic rocks in hand specimen and under the microscope (cross-polarized light). Py: Pyroxene; Pl: Plagioclase [Colour figure can be viewed at wileyonlinelibrary.com]

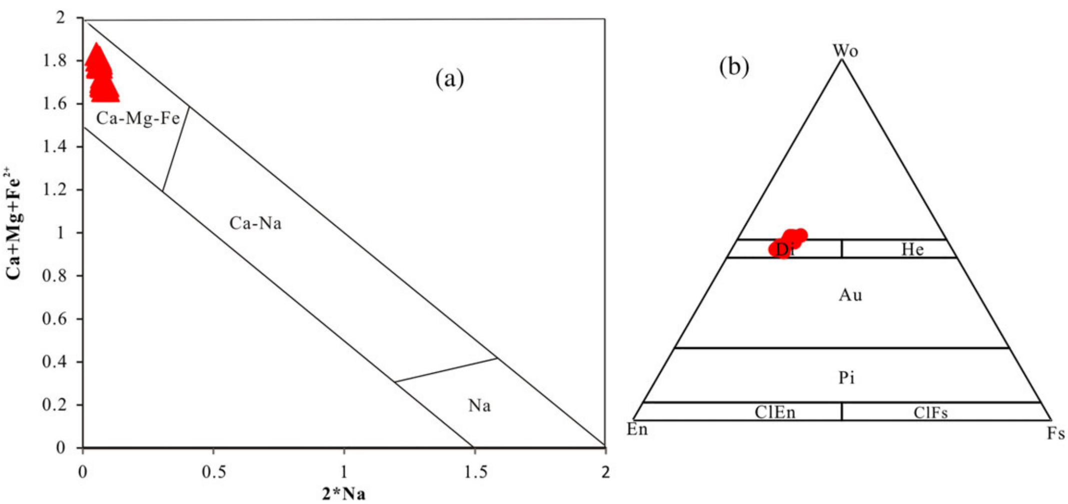

FIGURE 5 Diagram of Q-J series for clinopyroxenes (a) and diagram of classification for clinopyroxenes (after Morimoto, 1988). Di: diopside; He: hedenbergite; Au: Augite; Pi: Pigeonite; ClEn: clinoenstatite; ClFs: clinoferrosilite [Colour figure can be viewed at wileyonlinelibrary.com]

into eight major age ranges: 36 ± 1–33 ± 1 (eight grains), 116 ± 2–104 ± 1 (16 grains), 148 ± 4–140 ± 3 (two grains), 207 ± 2–196 ± 2 (three grains), 255 ± 7–236 ± 3 (three grains), 440 ± 7, 808 ± 10–749 ± 8 (three grains), and 2,440 ± 19–1,185 ± 29 Ma (three grains; Figure 7a, 8b). The first group gave a weighted mean $^{206}Pb/^{238}U$ age of 35.5 ± 0.9 Ma (MSWD = 1.7; Figure 7c,d).

These ~35-Ma zircons were prismatic and acicular, high length/width ratios (2–5). There were wide magmatic oscillatory zoning on the zircons. Moreover, the zircons have relatively high Th/U values (0.62–1.2), which were typical characteristics of zircons from volcanic rocks (Hoskin & Schaltegger, 2003; Wu & Zheng, 2004). Combining with regional tectonic evolution, we considered the age of 35.5 ± 0.9 Ma as the maximum eruption age of the basalts. Thirty-one grains yielded much older ages ranging from 2,468 to 106 Ma, which were inherited zircons crystallized from earlier magmas.

Xisha Uplift are far from the mainland, and their sedimentary diagenesis is less affected by terrigenous materials (Cao et al., 2016;

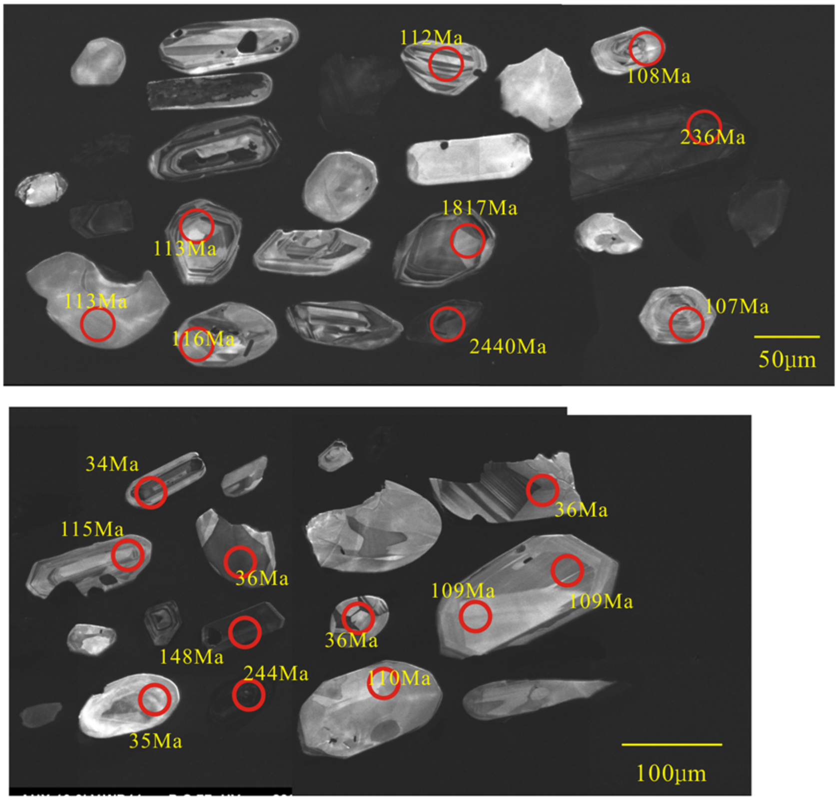

FIGURE 6 CL images of representative zircons. The approximate location of LA-ICP-MS analytical spot positions are marked with red circles

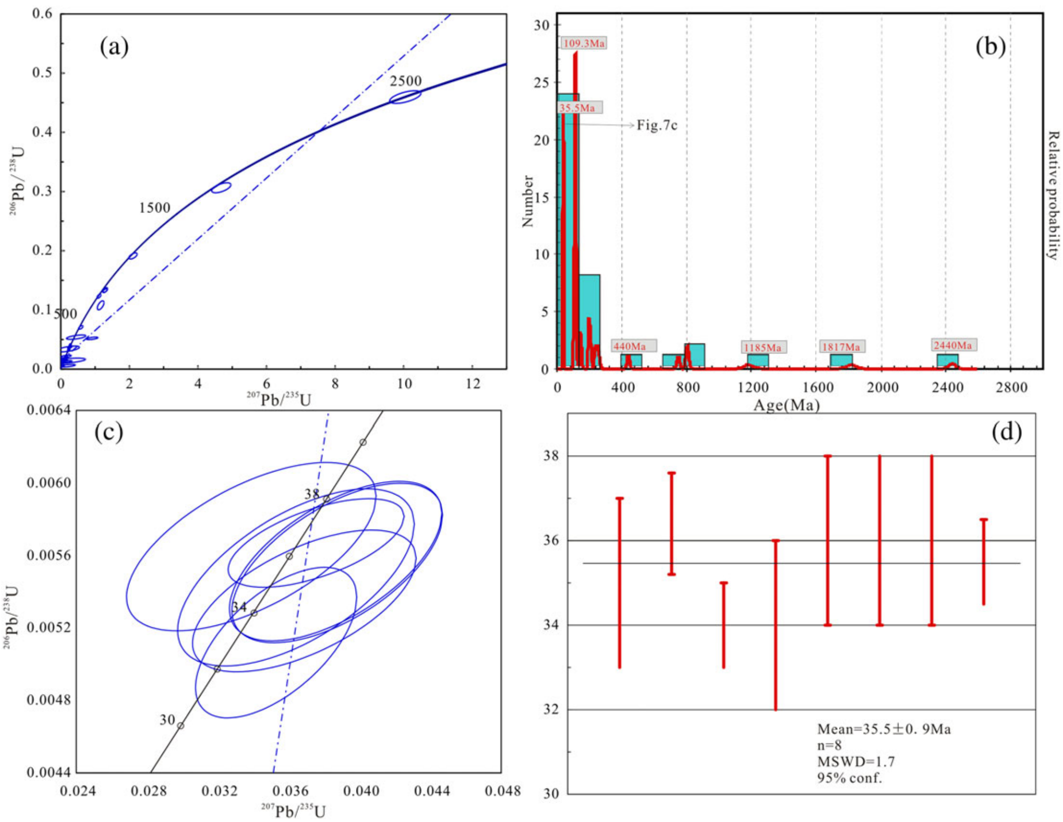

FIGURE 7 Zircon U–Pb concordia plot and weighted average $^{206}Pb/^{238}U$ age of the basaltic pyroclastic rocks from Well CK-2 [Colour figure can be viewed at wileyonlinelibrary.com]

Fang, Liu, Li, Zhang, & Ding, 2013; Lin et al., 2018). Tectonic subsidence research results show that the rapid subsidence of the basement in the Cenozoic formed three major sedimentary centres (Huaguang Depression, Changchang Depression, and Zhongjian Depression) around Xisha Uplift (Figure 2). These deep-water tectonic units prevent the terrigenous clastic sediments from the SCB and the

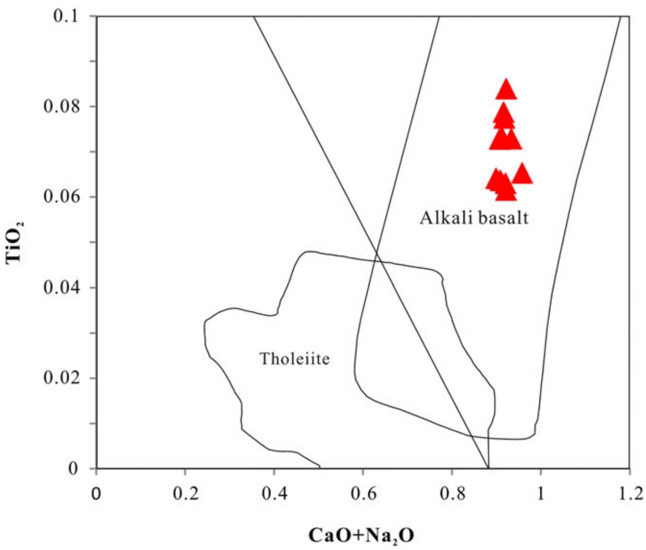

FIGURE 8 Ti–(Ca + Na) diagram of clinopyroxene of the basaltic pyroclastic rocks from Well CK-2 (after Leterrier et al., 1982) [Colour figure can be viewed at wileyonlinelibrary.com]

Indo-China peninsula being deposited in the Xisha Uplift and its surrounding slope areas (Yang et al., 2017). Furthermore, the results of petrographic studies show that the composition of volcanic clastic rocks is single and there is no mixing of terrestrial materials (such as quartz). All these evidence suggest that these old group zircon grains are inherited zircons rather than detrital zircons.

5 | DISCUSSION

5.1 | The alkaline magma and intraplate alkali basalt: Evidence from the clinopyroxene composition

The clinopyroxene is one of the main rock-forming minerals of mafic–ultramafic rocks. Clinopyroxene composition depends on primary magma characteristics and the crystallization environment. Its composition can well reflect the characteristics of the primary magma (Kargin, Sazonova, Nosova, & Tretyachenko, 2016; Leterrier, Maury, Thonon, Girard, & Marchal, 1982; Nisbet & Pearce, 1977; Rivalenti et al., 1996; Seyler & Bonatti, 1994; Tang et al., 2017). According to the mineral chemistry of clinopyroxene from Cenozoic basalts in the SCS, Yan, Shi, Wang, and Bu (2007) found that Pyroxene microlite has higher content in Ca, Ti, and Fe than pyroxene phenocryst and suggested that the evolution trend of host magma of pyroxene is coincidence with that of alkali rock series. In Ca + Na versus Ti discriminant diagram, all data from Well CK-2 are plotted into the field of alkaline basalt (Figure 8), indicating that the primary magma was the alkaline magma. As mentioned above, the clinopyroxenes showed high Al and Ti contents, which was consistent with the evolution trend of the alkaline magma.

Previous studies have demonstrated that the use of clinopyroxene can effectively determine the tectonic environment of basalt (Nisbet & Pearce, 1977; Yu, Zhao, Chen, Guo, & Wang, 2011). Nisbet and Pearce (1977) suggested that the major element of the clinopyroxene can be used to determine the tectonic setting. Yan et al. (2007) suggested that the Cenozoic basalt from SCS belonged to intraplate alkali basalt by using discriminant plot of clinopyroxene. The Cenozoic basalts may be products of the continuous evolution of the mantle plume (Yan et al., 2007). In F1–F2 discriminant diagram for tectonic setting (Figure 9), most of the data points from Well CK-2 basaltic pyroclastic rocks are plotted into the field of intraplate alkali basalt. In the TiO_2–Na_2O–MnO triangular diagram (Figure 10), all data points lie in the field of intraplate alkali basalt, which indicated that they lie at intraplate tectonic setting. In general, these basaltic pyroclastic rocks were characterized by the tectonic setting of the intraplate alkali basalt.

5.2 | The pyroclastic rocks were deposited as early as 35 Ma

Zircon grains have been found in a variety of basaltic rocks (Pan et al., 2014; Wang, Li, Xie, Xu, & Li, 2015; Yang, Chen, Hou, Liu, & Liu, 2014; Zhang et al., 2015). However, SiO_2 and ZrO_2 are normally unsaturated in basaltic rocks. Therefore, there are many controversies on the genesis of the zircon crystals in such magmas (Luo, Mo, Wan, & Wei, 2006; Zhang et al., 2013). The zircon in basaltic rocks may crystallize in a magma chamber or is captured from the wall rock when the magma is raised. In this research, the youngest group gave a weighted mean $^{206}Pb/^{238}U$ age of 35.5 ± 0.9 Ma (MSWD = 1.7), which may represent the maximum age of the basalt eruption. The youngest Eocene zircons either generated during the eruption of the basalt and consequently represent the eruption age of the basalts or might also be inherited from other early volcanic rocks, implying that the basaltic pyroclastic rocks formed later.

The petrographic studies show that the phenocrysts are subangular or angular and broken into steps or jagged shapes along

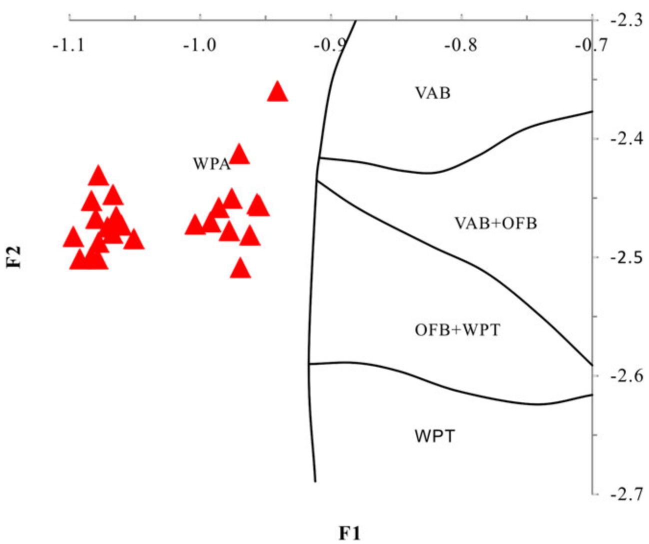

FIGURE 9 F1 versus F2 diagram of clinopyroxene (after Nisbet & Pearce, 1977) WPT: within-plate tholeiitic basalt; WPA: within-plate alkali basalt; VAB: volcanic arc basalt; OFB: ocean floor basalt F1 = 0.012 × SiO_2–0.0807 × TiO_2) + 0.0026 × Al_2O_3–0.0012 × FeO* – 0.0026 × MnO + 0.0087 × MgO – 0.0128 × CaO – 0.0419 × Na_2O; F2 = –0.0469 × SiO_2–0.0818 × TiO_2–0.0212 × Al_2O_3–0.0041 × FeO* – 0.1435 × MnO – 0.0029 × MgO + 0.0085 × CaO + 0.016 × Na_2O [Colour figure can be viewed at wileyonlinelibrary.com]

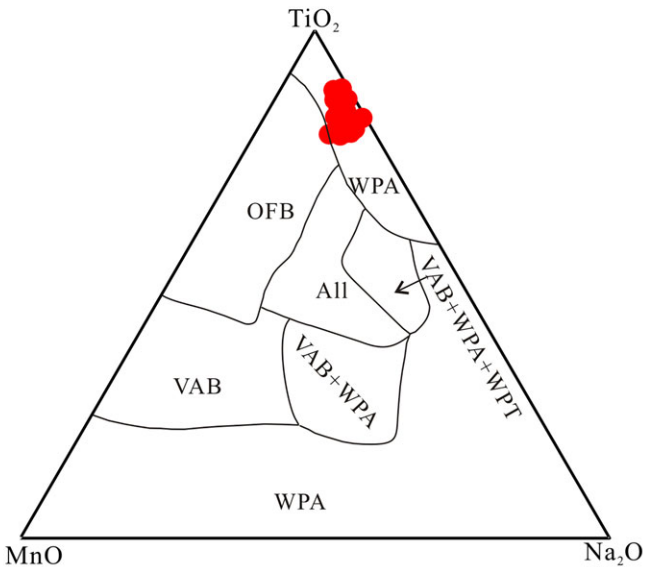

FIGURE 10 TiO_2–MnO–Na_2O diagram of clinopyroxene of the basaltic pyroclastic rocks from Well CK-2 (after Nisbet & Pearce, 1977). WPT: within-plate tholeiitic basalt; WPA: within-plate alkali basalt; VAB: volcanic arc basalt; OFB: ocean floor basalt [Colour figure can be viewed at wileyonlinelibrary.com]

the cleavage plane, suggesting the basaltic pyroclastic rocks are in situ or nearby volcanism (Figure 3). Furthermore, this suite of basaltic pyroclastic rocks is more than 50-m thick. If they are transported over long distances, they will be widely distributed in Xisha Islands. However, Well XK-1 and Well XY-1, which are located near to Well CK-2, drilled through the thick reefal limestone and into the underlying metamorphic basement. None of the two wells found pyroclastic rocks or terrigenous clastic rocks. Furthermore, the depocenter (Huaguang Depression, Changchang Depression, and Zhongjian Depression) around the Xisha Uplift prevent the exotic pyroclastic material from the SCB being deposited in the Xisha Uplift. Therefore, we suggest that the basaltic pyroclastic rocks are in situ or nearby volcanism. Sr isotopes from the carbonate rocks show that carbonate rocks began to develop from 19.6 Ma (unpublished data), indicating that the basaltic pyroclastic rocks may have been formed before 19.6 Ma. Combining with the zircon U–Pb ages, we suggest that the basaltic pyroclastic rocks might be formed in 35.5–19.6 Ma, indicating that there may be an alkaline magma activity during 35.5–19.6 Ma in Xisha Islands, which may be related to the expansion of the SCS.

5.3 | The volcanic activity in Xisha Islands

As indicated by gravitational and magnetic anomalies, igneous rocks are considered to be widely distributed in the Xisha Islands (Ma et al., 2016; Wan et al., 2006). Ma et al. (2011) pointed out that there were two periods of volcanic activity in Xisha Islands. Based on the latest high-resolution multichannel seismic data in combination with drilling well data, the Cenozoic magmatism of Xisha Islands are divided into the three periods: Palaeocene and Eocene, early Oligocene to mid-Miocene, and mid-Miocene to Recent (Zhang, 2014; Zhang et al., 2014; Zhang, Wu, & Dong, 2016). Extrusive structures are divided into flat-topped and conical-topped seamounts (Zhang et al., 2014; Zhang et al., 2016). The remarkable characteristics of the flat-topped seamount are flat and broad top and steep slope. There are 13 flat-topped seamounts in Xisha sea area (Zhang, 2014). Generally, the maximum width on the top of the flat-topped seamount is more than 8 km. Magnetic anomaly suggests that the flat-topped seamount might be of basaltic nature rather than continental crust or shallow water sandstone deposits. The conical-topped seamounts are considered to be formed in a strong central volcanic eruption. They are mainly distributed along the large fault in a beaded shape. Compared with flat-topped seamounts, the conical-topped seamounts have a high and sharp head, which is exposed above seafloor (Zhang, 2014; Zhang et al., 2014; Zhang et al., 2016). As the only volcanic island exposed in Xisha sea area, the K–Ar age of volcanic rocks from Gaojianshi Island is 1.57 Ma (Zou, 1993).

Huang, Qiu, Xu, and Zeng (2011) used natural seismic data from Chenhang Island to simulate the crustal structure and found that the lower crust had a ductile rheological structure caused by the deep thermal activity of the mantle. Due to the multiphase expansion of the SCS, the Xisha Islands are characterized by thin continental crust, and there are extensive deep faults around the periphery, which are prone to volcanic activity. Seismic data show that there are NE-ENE and NW trending faults along the Xisha block boundary. The reactivation of the faults accompanied by volcanicity is affected by multiphase tectonic movements (Feng et al., 2015). Based on seismic data, Feng et al. (2017) further pointed out that there are multiple volcanic structures in Xisha sea area.

The basaltic pyroclastic rocks in this study indicate that there have been explosive volcanic activities in Xisha sea area in the SCS. Combining the characteristics of the basaltic pyroclastic rocks and the volcanic activity in Xisha Islands, we further speculate that Chenhang Island had volcanic activity. It may be one of the 13 flat-topped seamounts described by Zhang (2014). Pyroclastic rock on seamount is the product of explosive volcanism (Yan & Shi, 2007). Due to the positive topography of the top of the seamount, it is difficult for the exogenous debris to reach the top of the seamount. Therefore, the source region of basaltic pyroclastic rocks is relatively simple, except for a small amount of biological remains carried in suspension manner. Since the Miocene, subsidence has occurred in the whole region of Xisha Islands, which has been gradually submerged by sea water. As a result, this region has suitable temperature, salinity, and water depth, and coral reef carbonate strata have been extensively developed. Unfortunately, our drilling did not drill through the pyroclastic rock. Thus, more drilling and geophysical data are needed to prove this speculation.

5.4 | Comparison of tectono-magmatic event around the SCS

Generally, most of the zircon grains from basaltic rocks are considered as inherited zircons, which were derived from the crustal section and traversed by the host lava (Pan et al., 2014). Thus, inherited zircons can be used to indicate the concealed magma event (Condie, Belousova, Griffin, & Sircombe, 2009; Pereira et al., 2011). The ages of the zircon grains are basically consistent with the main magmatism events in the SCB (Wang, Fan, Zhang, & Zhang, 2013; Wang, Yu, Griffin, & O'Reilly, 2012), suggesting that they may be related to magmatic events in the SCB.

The second group of the zircons yielded an average age of 109.3 Ma (116–104 Ma, 16 grains). There are only two zircon grains in the third group, with an average age of 144 Ma (148–144 Ma, two grains). The two group zircons may derive from hidden magmatic intrusions, which record two major igneous activities in the SCS. The contemporaneous granitic rocks are widely distributed surrounding the SCS region, such as Pearl River Mouth Basin, Zhongsha Block, Nansha Block, and Xisha block. The Late Mesozoic magmatic activity in the SCS continued over a long period of time, ranging from 159 to 70.5 Ma (Yan, Shi, & Castillo, 2014; Zhu et al., 2017). It is generally believed that the Late Mesozoic igneous activity are the result of the subduction of the old Pacific Plate beneath the Eurasian Plate (Yan, Li, & Yan, 2014 and references therein). The ages of the granitic rocks from the Nansha microblock vary from 159 to 127 Ma (Yan et al., 2010). Well XK-1, which is located in Shidao, Xisha Islands, is near to Well CK-2. The basement rocks of the Well XK-1 consist of amphibole plagiogneisses and the granite. The granitic rocks have an average zircon $^{206}Pb/^{238}U$ age of 107.8 ± 3.6 Ma. The zircon grains of magmatic origin from the amphibole plagiogneisses yielded an average age of 152.9 ± 1.7 Ma, hinting that the protolith of the gneisses was the Late Jurassic igneous rocks (Zhu et al., 2017). These two zircon U–Pb ages are similar to our research, indicating that there may be a genetic link. In other words, they may record similar igneous activity. The Yanshanian tectono-magmatic events that extensively affected the South China Block (SCB) during the Mesozoic may also involve the microcontinental block scattered in the SCS.

Six zircon grains display scattered Early Mesozoic ages (Group 4 and Group 5, 255–196 Ma), which records the Indosinian magmatic activity. The South China Indosinian granites are mainly distributed in South China inland, which were the results of the subduction–collision–extension processes of the surrounding blocks (Mao et al., 2013; Mao, Li, & Ye, 2014). There are two stages of early Mesozoic granites, whose age ranges are 228–244 and 210–218 Ma, respectively (Song, Shu, Santosh, & Li, 2015; Wang et al., 2013). Thus, the magmatic events represented by the inherited zircons of in this study are in good agreement with the Indosinian magmatic activities in the SCB, suggesting that there may be a causal relationship. These magmatic activities were the products of the convergence of multiple blocks (Mao et al., 2014).

There is only one Early Palaeozoic zircon grain in this study. The corresponding magmatic rocks (440–309 Ma) are exposed extensively in the SCB (Zhou, Sun, Shen, Shu, & Niu, 2006; Wang et al., 2011, 2013). Most of the Early Palaeozoic magmatic rocks were granitic rocks, which mainly distributed in the Cathaysia Block. The corresponding magmatic events have been interpreted as related intracontinental orogeny triggered by interactions between the Yangtze and Cathaysia continental blocks (Song et al., 2015).

In the studied sample, only three grains have Neoproterozoic ages (808–749 Ma). The Neoproterozoic-exposed rocks (808–749 Ma) recently have been identified in the eastern segment of Wuyi-Yunkai orogen in SCB (Li et al., 2010; Li, Li, Li, & Liu, 2008). These magmatic events used to be interpreted as related to the mantle superplume, which led the breakup of the supercontinent Rodinia (Li et al., 2008; Wang & Li, 2003; Yu et al., 2008). However, Xiu et al. (2017) suggested that the SCB was located on the margin of Rodinia supercontinent and rule out mantle plume in SCB. Furthermore, Neoproterozoic inherited zircon (675 Ma) has been found from granitic rocks in Nansha microblock, indicating the presence of Proterozoic components in the source regions of the magma (Yan, Shi, Wang, & Liu, 2008, 2010).

The 1,185 Ma corresponds to the Grenville Orogeny. The Mesoproterozoic ages have also been found in detrital zircons and inherited zircons in the southern Cathaysia Block (Xiang & Shu, 2010; Wang, Yu, Griffin, & O'Reilly, 2008 and reference therein). There was a young Grenville-aged Orogeny in the southern Cathaysia Block, which is different with Jiangnan Orogen along the southeastern margin of the Yangtze Block (Wang et al., 2008; Xiang & Shu, 2010; Yu et al., 2007, 2008).

There are two Paleoproterozoic zircon grains in our study (1817 ± 28 and 2440 ± 19 Ma), which is the first report on Paleoproterozoic material in the SCS. The similar Paleoproterozoic ages have also been found in the SCB (Li, Li, & Li, 2014; Liu et al., 2014; Wang et al., 2008; Xiang et al., 2008; Xiang & Shu, 2010; Xu et al., 2007; Yu et al., 2007, 2008, 2010; Yu, O'Reilly, Zhou, Griffin, & Wang, 2012; Yu, Wang, O'Reilly, Shu, & Sun, 2009; Zheng et al., 2008; Zheng et al., 2011). The ~2.5 Ga corresponds to globally continental nuclei growth. The ~1.8-Ga tectonothermal event was synchronous with the assembly of the Columbia supercontinent. The Archaic information of the Cathaysia Block is currently only found in detrital zircons and inherited zircon cores. The provenance of the ~2.5-Ga zircon grains are controversial. Many geologists suggested that these zircons were from the unexposed Archean basement rocks (Shu, 2012; Xia, Xu, & Zhu, 2012; Xu et al., 2007; Yu et al., 2007, 2010; Zheng et al., 2011) and speculated the existence of the Archean crust at depth in the Cathaysia Block. However, no Archean rocks have been identified so far. The Badu Complex is generally considered to be a series of Paleoproterozoic strata, which may represent the oldest rocks known in the Cathaysia Block. The zircon U–Pb ages suggest that the Badu Complex were deposited at 2.5 Ga (Yu et al., 2012). Because the Archean detrital zircons are oval in shape with abrasive imprints, Li, Li, and Li (2014) suggested that the Archean detrital zircons were derived from East Antarctica rather than from Cathaysia itself (Li, Li, & Li, 2014). There may be no Archaean basement in the Cathaysia Block.

In general, the ages of inherited zircons are comparable to magmatic activities occurred around the SCS, implying the microcontinents dispersed in the SCS are of affinity with the SCB (Liu et al., 2006; Liu, Zhao, Fan, & Chen, 2002; Yan et al., 2010; Yan, Shi, Wang, et al., 2008). In other words, these microcontinents were probably once contiguous with the SCB (Yao et al., 2004). Due to the extension and thinning of the continental lithosphere of the SCS since the Late Cretaceous, these microcontinents began to rotate and displace, finally reaching the present position (Liu et al., 2004). The SCB, together with those continental terranes of east and Southeast Asia, are considered as an integrated part of Gondwana (Li et al., 2018; Li, Li, & Li, 2014; Yao, Li, Li, Li, & Yang, 2014; Yu et al., 2008). In all, all the above cases indicate that the SCS have Precambrian materials, and the ancient continental basement has experienced multistages magmatic events.

6 | CONCLUSIONS

1. This paper reports the basaltic pyroclastic rocks from Well CK-2, Xisha Islands, the northwestern SCS. The clinopyroxenes from the basaltic pyroclastic rocks were characterized by high content in Al and Ti and belonged to diopside. The primary magma was the alkaline magma and probably formed in an intraplate alkali basalt setting.
2. The youngest group yielded an age of 35.5 ± 0.9 Ma, which represents the maximum age of the basalt eruption.
3. The ages of inherited zircons were comparable to magmatic activities occurred around the SCS. The microcontinents dispersed in the SCS were of affinity with the SCB. This basaltic pyroclastic rock comprises one zircon grain forming at 2440 Ma, which is the oldest materials found in the SCS, indicating that the SCS basement may contain very old materials. The ancient continental basement has experienced multi-stages magmatic events.

ACKNOWLEDGEMENTS

This work was funded by the Natural Science Foundation of China (Grant 91428203), the Guangxi University (XBZ170339), Education Department of Guangxi Zhuang Autonomous Region (2018KY0045), Science and Technology Department of Guangxi Zhuang Autonomous Region (AD17129063 and AA17204074). We are grateful to two anonymous reviewers who provided constructive suggestions which led to improvement of the paper.

ORCID

Yu Zhang https://orcid.org/0000-0002-6537-8413

REFERENCES

Andersen, T. (2002). Correction of common lead in U-Pb analyses that do not report ^{204}Pb. *Chemical Geology*, *192*, 59–79.

Cao, J. Q., Zhang, D. J., Zhai, S. K., Luo, W., Xiu, C., Liu, X. Y., … Bi, D. J. (2016). The characteristics and genetic model of the dolomitization in Xisha Reef Islands. *Acta Oceanologica Sinica*, *38*(11), 125–139. (in Chinese with English abstract)

Condie, K. C., Belousova, E., Griffin, W. L., & Sircombe, K. N. (2009). Granitoid events in space and time: Constraints from igneous and detrital zircon age spectra. *Gondwana Research*, *15*(3–4), 228–242.

Ding, W. W., & Li, J. B. (2016). Conjugate margin pattern of the Southwest Sub-basin, South China Sea: Insights from deformation structures in the continent-ocean transition zone. *Geological Journal*, *51*(S1), 524–534.

Fang, N. Q., Liu, H., Li, Q., Zhang, W., & Ding, X. (2013). The pattern of carbonate sedimention and its relation the evolution of the South China Sea in Cenozoic. *Earth Science Frontiers*, *20*(5), 227–234. (in Chinese with English abstract)

Fang, P., Ding, W., Fang, Y., Zhao, Z., & Feng, Z. (2016). Cenozoic tectonic subsidence in the southern continental margin, South China Sea. *Frontiers of Earth Science*, *11*(2), 427–441.

Feng, Y. C., Zhan, W. H., Sun, J., Yao, Y. T., Guo, L., & Chen, M. (2017). The formation mechanism and characteristics of volcanoes in the Xisha waters since Pliocene. *Journal of Tropical Oceanography*, *36*(3), 73–79. (in Chinese with English abstract)

Feng, Y. C., Zhan, W. H., Yao, Y. T., Sun, J., Liu, S. J., & Li, J. (2015). Analysis of tectonic movement and activity in the organic reef region around the Xisha Islands. *Journal of Tropical Oceanography*, *34*(3), 48–53. (in Chinese with English abstract)

Franke, D. (2013). Rifting, lithosphere breakup and volcanism: Comparison of magma-poor and volcanic rifted margins. *Marine and Petroleum Geology*, *43*(3), 63–87.

Guo, L. L., Li, S. Z., Zhao, S. J., Zhang, G. X., Suo, Y. X., Liu, H., … Wang, Q. (2016). Final breakup of continental block and opening of oceanic lithosphere: insights from deep crustal structure and tectonic evolution of the ocean–continent transition zone in the northern South China Sea. *Geological Journal*, *51*(S1), 318–330.

Hoskin, P. W. O., & Ireland, T. R. (2000). Rare earth element chemistry of zircon and its use as a provenance indicator. *Geology*, *28*, 627–630.

Hoskin, P. W. O., & Schaltegger, U. (2003). The composition of zircon and igneous and metamorphic petrogenesis. *Reviews in Mineralogy and Geochemistry*, *53*, 27–62.

Hsieh, R. B. J., Shellnutt, J. G., & Yeh, M. W. (2016). Age and tectonic setting of the East Taiwan Ophiolite: Implications for the growth and development of the South China Sea. *Geological Magazine*, *154*(3), 441–455.

Huang, H. B., Qiu, X. L., Xu, Y., & Zeng, G. P. (2011). Crustal structure beneath the Xisha Islands of the South China Sea simulated by the teleseismic receiver function method. *Chinese Journal of Geophysics*, *54*(11), 2788–2798. (in Chinese with English abstract)

Huang, X. L., Niu, Y. L., Xu, Y. G., Ma, J. L., & Qiu, H. N. (2013). Geochronology and geochemistry of Cenozoic basalts from eastern Guangdong, SE China: Constraints on the lithosphere evolution beneath the northern margin of the South China Sea. *Contributions to Mineralogy and Petrology*, *165*(3), 437–455.

Hui, G. G., Li, S. Z., Li, X. Y., Guo, L. L., Suo, Y. H., Somerville, I. D., … Zhang, J. (2016). Temporal and spatial distribution of Cenozoic igneous rocks in the South China Sea and its adjacent regions: Implications for tectono-magmatic evolution. *Geological Journal*, *51*(S1), 429–447.

Hui, G. G., Li, S. Z., Li, X. Y., Zhang, G. X., Gong, Y. H., Somerville, I. D., … Zang, Y. B. (2016). Source and accumulation of gas hydrate in the northern margin of the South China Sea. *Marine and Petroleum Geology*, *69*, 127–145.

Kargin, A. V., Sazonova, L. V., Nosova, A. A., & Tretyachenko, V. V. (2016). Composition of garnet and clinopyroxene in peridotite xenoliths from the Grib kimberlite pipe, Arkhangelsk diamond province, Russia: Evidence for mantle metasomatism associated with kimberlite melts. *Lithos*, *262*, 442–455.

Lei, J. P., Jiang, S. H., Li, S. Z., Gao, S., Zhang, H. X., Wang, G., & Zhao, F. Y. (2016). Gravity anomaly in the southern South China Sea: A connection of Moho depth to the nature of the sedimentary basins' crust. *Geological Journal*, *51*(S1), 244–262.

Leterrier, J., Maury, R. C., Thonon, P., Girard, D., & Marchal, M. (1982). Clinopyroxene composition as a method of identification of the magmatic affinities of paleovolcanic series. *Earth and Planetary Science Letters*, *59*, 139–154.

Li, C. F., Li, J. B., Ding, W. W., Franke, D., Yao, Y., Shi, H., … Zhang, G. (2015). Seismic stratigraphy of the central South China Sea basin and implications for neotectonics. *Journal of Geophysical Research - Solid Earth*, *120*(3), 1377–1399.

Li, N. S., Yan, Q. S., Chen, Z. H., & Shi, X. F. (2013). Geochemistry and petrogenesis of Quaternary volcanism from the islets in the eastern Beibu Gulf: Evidence for Hainan plume. *Acta Oceanologica Sinica*, *32*(12), 40–49.

Li, S. Z., Suo, Y. H., Li, X. Y., Liu, B., Dai, L. M., Wang, G. Z., … Zhang, G. W. (2018). Microplate tectonics: New insights from micro-blocks in the global oceans, continental margins and deep mantle. *Earth-Science Reviews*, *185*, 1029–1064.

Li, X., Li, J., Yu, X., Wang, C. S., & Jourdan, F. (2015). ^{40}Ar/^{39}Ar ages of seamount trachytes from the South China Sea and implications for the evolution of the northwestern sub-basin. *Geoscience Frontiers*, *6*(4), 571–577.

Li, X. H., Li, W. X., Li, Z. X., & Liu, Y. (2008). 850–790 Ma bimodal volcanic and intrusive rocks in northern Zhejiang, South China: A major episode of continental rift magmatism during the breakup of Rodinia. *Lithos*, *102*(1), 341–357.

Li, X. H., Li, Z. X., & Li, W. X. (2014). Detrital zircon U-Pb age and Hf isotope constrains on the generation and reworking of Precambrian continental crust in the Cathaysia Block, South China: A synthesis. *Gondwana Research*, *25*(3), 1202–1215.

Li, Z. X., Li, X. H., Wartho, J. A., Clark, C., Li, W. X., Zhang, C. L., & Bao, C. (2010). Magmatic and metamorphic events during the Early Paleozoic Wuyi–Yunkai Orogeny, southeastern South China: New age constraints and pressure–temperature conditions. *Geological Society of America Bulletin*, *122*, 772–793.

Lin, W. H., Yu, K. F., Wang, Y. H., Liu, X. M., Wang, J. J., Ning, Q. Y., & Li, Y. H. (2018). Extremely low radioactivity in marine sediment of coral reefs and its mechanism. *Chinese Science Bulletin*, *63*, 2173–2183. (in Chinese with English abstract)

Liu, H., Luan, X. W., Guo, L. L., Yue, B. J., Zhang, L., Ran, W. M., & Pan, J. (2016). Fault distribution and formation mechanism of a magnetic quiet zone in the northern South China Sea. *Geological Journal*, *51*(S1), 331–345.

Liu, H. L., Yan, P., Liu, Y. C., & Deng, H. (2006). Discussion on the existence of Qiongnan suture in the northern margin of the South China Sea and its implications. *Chinese Science Bulletin*, *51*(Suppl), 92–101. (in Chinese)

Liu, H. L., Yang, T., Zhu, S. G., Zhang, N. Y., Qiu, X. L., & Shi, X. B. (2004). Tectonic evolution of Cenozoic sedimentary basements in the northwestern South China Sea. *Acta Oceanologica Sinica*, *26*(3), 54–67. (in Chinese with English abstract)

Liu, J. H., Liu, D. Y., Zhang, Y. H., & Yang, Z. Q. (2011). Techniques for choosing target points during SHRIMP dating of zircon U–Pb ages. *Rock Mineral Anal*, *30*(3), 265–268. (in Chinese with English abstract)

Liu, Q., Yu, J. H., O'Reilly, S. Y., Zhou, M. F., Griffin, W. L., Wang, L. J., & Cui, X. (2014). Origin and geological significance of Paleoproterozoic granites in the northeastern Cathaysia Block, South China. *Precambrian Research*, *48*(7), 72–95.

Liu, Y. S., Gao, S., Hu, Z. C., Gao, C. G., Zong, K. Q., & Wang, D. B. (2010). Continental and oceanic crust recycling-induced melt-peridotite interactions in the Trans-North China Orogen: U-Pb dating, Hf isotopes and trace elements in zircons of mantle xenoliths. *Journal of Petrology*, *51*(1–2), 537–571.

Liu, Z. S., Zhao, H. T., Fan, S. Q., & Chen, S. Q. (2002). *Geology of the South China Sea* (pp. 1–5). Beijing, China: Science Press.

Lu, B. L., Sun, X. M., Zhang, G. C., Zhang, B., Lang, Y. Q., & Wang, P. J. (2011). Seismic-potential field response characteristics and identification of basement lithology of the northern South China Sea basin. *Chinese Journal of Geophysics*, *54*(2), 563–572. (in Chinese with English abstract)

Lü, C. C., Hao, T. Y., Yao, Y. J., Xing, J., & Qiu, X. L. (2016). Oceanic mantle gravimetric response to the seafloor spreading of the southwest sub-basin, South China Sea. *Geological Journal*, *51*(S1), 535–547.

Ludwig, K. R. (2003). *ISOPLOT 3.00: A geochronological toolkit for Microsoft Excel*. Berkeley: Berkeley Geochronology Center, California.

Luo, Z. H., Mo, X. X., Wan, Y. S., & Wei, Y. (2006). Geological implications of the youngest SHRIMP U-Pb age of the alkaline basalt in the Tibetan Plateau. *Acat Petrologica Sinica*, *22*(3), 578–584. (in Chinese with English abstract)

Ma, Y., Li, S. Z., Lin, J. Q., Liang, Q. Y., Shi, Y. H., & Kong, L. (2016). Magma emplacement: An important trigger leading to slope failures in deep-water areas of northern continental margin of South China Sea. *Geological Journal*, *51*(S1), 96–107.

Ma, Y. B., Wu, S. G., Lv, F. L., Dong, D. D., Sun, Q. L., Lu, Y. T., & Gu, M. F. (2011). Seismic characteristics and development of the Xisha carbonate platforms, northern margin of the South China Sea. *Journal of Asian Earth Sciences*, *40*(3), 770–783.

Mao, J. R., Li, Z. L., & Ye, H. M. (2014). Mesozoic tectono-magmatic activities in South China: Retrospect and prospect. *Science China: Earth Sciences*, *57*, 2853–2877.

Mao, J. R., Ye, H. M., Liu, K., Li, Z. L., Takahashi, Y., Zhao, X. L., & Kee, W. S. (2013). The Indosinian collision-extension event between the South China Block and the Palaeo-Pacific plate: Evidence from Indosinian alkaline granitic rocks in Dashuang, eastern Zhejiang, South China. *Lithos*, *172*(4), 81–97.

Morimoto, N. (1988). Nomenclature of pyroxenes. *Mineralogy and Petrology*, *39*, 55–76.

Nisbet, E. G., & Pearce, J. A. (1977). Clinopyroxene composition in mafic lavas from different tectonic settings. *Contributions to Mineralogy and Petrology*, *63*(2), 149–160.

Pan, S. K., Zheng, J. P., Griffin, W. L., Chu, L. L., Xu, Y. X., Li, Y. L., … Wang, D. (2014). Precambrian tectonic attribution and evolution of the Songliao terrane revealed by zircon xenocrysts from Cenozoic alkali basalts, Xilinhot region, NE China. *Precambrian Research*, *251*, 33–48.

Pereira, M. F., Chichorro, M., Solá, A. R., Silva, J. B., Sánchez-García, T., & Bellido, F. (2011). Tracing the Cadomian magmatism with detrital/inherited zircon ages by in-situ U-Pb SHRIMP geochronology (Ossa Morena Zone, SW Iberian Massif). *Lithos*, *123*(1–4), 204–217.

Qin, G. Q. (1987). Apreliminary study on foraminifer assemblages of Well 1 Xiyong, Xisha islands and their coral reef formation. *Trophic Oceanology*, *6*(3), 10–20. (in Chinese)

Rivalenti, G., Vannucci, R., Rampone, E., Mazzucchelli, M., Piccardo, G. B., Piccirillo, E. M., & Ottolinib, L. (1996). Peridotite clinopyroxene chemistry reflects mantle processes rather than continental versus oceanic settings. *Earth and Planetary Science Letters*, *139*(3–4), 423–437.

Seyler, M., & Bonatti, E. (1994). Na, Al^{IV} and Al^{VI} in clinopyroxenes of subcontinental and suboceanic ridge peridotites: A clue to different melting processes in the mantle. *Earth and Planetary Science Letters*, *122*(3–4), 281–289.

Shi, X. F., & Yan, Q. S. (2011). Geochemistry of Cenozoic magmatism in the South China Sea and its tectonic implications. *Marine Geology & Quaternary Geology*, *31*(2), 59–72. (in Chinese with English abstract)

Shu, L. S. (2012). An analysis of principal features of tectonic evolution in South China Block. *Geological Bulletin of China*, *31*(7), 1035–1053. (in Chinese with English abstract)

Song, M., Shu, L., Santosh, M., & Li, J. L. (2015). Late Early Paleozoic and Early Mesozoic intracontinental orogeny in the South China Craton: Geochronological and geochemical evidence. *Lithos*, *232*, 360–374.

Sun, J. S. (1987). A discussion of the formation ages of the bed rock in the Xisha Islands. *Marine Geology and Quaternary Geology*, *7*(4), 5–6. (in Chinese)

Tang, D. M., Qin, K. Z., Chen, B., Mao, Y. J., Guo, H., & Evans, N. J. (2017). Mineral chemistry and genesis of the Permian Cihai and Cinan magnetite deposits, Beishan, NW China. *Ore Geology Reviews*, *86*, 79–99.

Taylor, B., & Hayers, D. E. (1983). The tectonic evolution of the South China Sea. In D. E. Hayers (Ed.), *The tectonic and geological evolution of the Southeast Asian seas and islands, 1* (pp. 23–56). Washington, DC: American Geophysical Union.

Wan, L., Yao, B. C., Zeng, W. J., Wu, N. Y., Xia, B., & Zhu, B. D. (2006). Lithospheric structure and petroleum distribution in the South China Sea. *Geology in China*, *33*(4), 874–884. (in Chinese with English abstract)

Wang, J., & Li, Z. X. (2003). History of Neoproterozoic rift basins in South China: Implications for Rodinia breakup. *Precambrian Research*, *122*, 141–158.

Wang, J., Zhao, M. G., Qiu, X. L., Sibuet, J. C., He, E. Y., Zhang, J. Z., & Tao, C. H. (2016). 3D seismic structure of the Zhenbei–Huangyan seamounts chain in the East Sub-basin of the South China Sea and its mechanism of formation. *Geological Journal*, *51*(S1), 448–463.

Wang, L. J., Yu, J. H., Griffin, W. L., & O'Reilly, S. Y. (2008). Grenvillian orogeny in the Southern Cathaysia Block: Constraints from U-Pb ages and Lu-Hf isotopes in zircon from metamorphic basement. *Chinese Science Bulletin*, *53*(19), 3037–3050.

Wang, L. J., Yu, J. H., Griffin, W. L., & O'Reilly, S. Y. (2012). Early crustal evolution in the western Yangtze Block: Evidence from U-Pb and LuHf isotopes on detrital zircons from sedimentary rocks. *Precambrian Research*, *222–223*, 368–385.

Wang, M., Li, C., Xie, C. M., Xu, J. X., & Li, X. K. (2015). U-Pb zircon age, geochemical and Lu–Hf isotopic constraints of the Southern Gangma Co basalts in the Central Qiangtang, northern Tibet. *Tectonophysics*, *657*, 219–229.

Wang, R., Yu, K. F., Jones, B., Wang, Y. H., Zhao, J. X., Feng, Y. X., … Zhang, Y. (2018). Evolution and development of Miocene "island dolostones" on Xisha Islands, South China Sea. *Marine Geology*, *406*, 142–158.

Wang, Y. J., Fan, W. M., Zhang, G. W., & Zhang, Y. H. (2013). Phanerozoic tectonics of the South China Block: Key observations and controversies. *Gondwana Research*, *23*(4), 1273–1305.

Wang, Y. J., Zhang, A. M., Fan, W. M., Zhao, G. C., Zhang, G. W., Zhang, Y. Z., … Li, S. Z. (2011). Crustal anatexis in an intracontinental regime: Geochemical, zircon U–Pb geochronological and Hf isotopic fingerprints from the middle Paleozoic (Kwangsian) gneissoid granites in the eastern South China Block. *Lithos*, *127*, 239–260.

Wu, Y. B., & Zheng, Y. F. (2004). Genesis of zircon and its constraints on interpretation of U-Pb age. *Chinese Science Bulletin*, *49*(15), 1554–1569.

Xia, Y., Xu, X. S., & Zhu, K. Y. (2012). Paleoproterozoic S- and A-type granites in southwestern Zhejiang: Magmatism, metamorphism and implications for the crustal evolution of the Cathaysia basement. *Precambrian Research*, *216–219*, 177–207.

Xiang, H., Li, Z., Zhou, H. W., Zhong, Z. Q., Zeng, W., Liu, R., & Jing, S. (2008). U-Pb zircon geochronology and Hf isotope study of metamorphosed basic-ultrabasic rocks from metamorphic basement in southwestern Zhejiang: The response of the Cathaysia Block to Indosinian orogenic even. *Science in China Series D: Earth Sciences*, *51*(6), 788–800.

Xiang, L., & Shu, L. S. (2010). Pre-Devonian tectonic evolution of the eastern South China Block: Geochronological evidence from detrital zircons. *Science China Earth Sciences*, *53*, 1427–1444.

Xie, A. Y., Zhong, L. F., & Yan, F. (2017). Time and genesis of Cenozoic magmaticcs in the South China Sea and surrounding areas. *Marine Geology and Quaternary Geology*, *37*(2), 108–118. (in Chinese with English abstract)

Xiu, C., Zhang, D. J., Zhai, S. K., Liu, X. Y., Cao, J. Q., Bi, D. J., & Chen, K. (2017). REE geochemical characteristics and diagenetic environments of reef dolostone in Shi Island, Xisha Islands. *Marine Science Bulletin*, *36*(2), 151–167.

Xu, J. Y., Avraham, Z. B., Kelty, T., & Yu, H. S. (2014). Origin of marginal basins of the NW Pacific and their plate tectonic reconstructions. *Earth-Science Reviews*, *130*, 154–196.

Xu, S. M., Ye, Q., Li, S. Z., Somerville, I., Feng, H. W., Tang, Z. W., … Bi, H. M. (2016). Sequential patterns in Cenozoic marginal basins of the Northwest Pacific. *Geological Journal*, *51*(S1), 387–415.

Xu, X. S., O'Reilly, S. Y., Griffin, W. L., Wang, X. L., Pearson, N. J., & He, Z. Y. (2007). The crust of Cathaysia: Age, assembly and reworking of two terranes. *Precambrian Research*, *158*(1–2), 51–78.

Xu, Y. G., Wei, J. X., Qiu, H. N., Zhang, H. H., & Huang, X. L. (2012). Opening and evolution of the South China Sea constrained by studies on volcanic rocks: Preliminary results and a research design. *Chinese Science Bulletin*, *57*(24), 3150–3164.

Yan, J. Y., Li, X. P., & Yan, Q. S. (2014). Geochemical characteristics and geological implications of clinopyroxenes in Cenozoic basalts from the South China Sea. *Geological Review*, *60*(4), 824–838. (in Chinese with English abstract)

Yan, P., Deng, H., Liu, H. L., Zhang, Z. R., & Jiang, Y. K. (2006). The temporal and spatial distribution of volcanism in the South China Sea region. *Journal of Asian Earth Sciences*, *27*(5), 647–659.

Yan, Q. S., Castillo, P., Shi, X. F., Wang, L. L., Liao, L., & Ren, J. B. (2015). Geochemistry and petrogenesis of volcanic rocks from Daimao Seamount (South China Sea) and their tectonic implications. *Lithos*, *218*, 117–126.

Yan, Q. S., & Shi, X. F. (2007). Hainan mantle plume and the formation and evolution of the South China Sea. *Geological Journal of China Universities*, *13*(2), 311–322. (in Chinese with English abstract)

Yan, Q. S., Shi, X. F., & Castillo, P. R. (2014). The late Mesozoic-Cenozoic tectonic evolution of the South China Sea: A petrologic perspective. *Journal of Asian Earth Sciences*, *85*, 178–120.

Yan, Q. S., Shi, X. F., Liu, J. H., Wang, K. S., & Bu, W. R. (2010). Petrology and geochemistry of Mesozoic granitic rocks from the Nansha micro-block, the South China Sea: Constraints on the basement nature. *Journal of Asian Earth Sciences*, *37*(2), 130–139.

Yan, Q. S., Shi, X. F., Wang, K. S., & Bu, W. R. (2007). Mineral chemistry and its genetic significance of olivine in Cenozoic basalts from the South China Sea. *Acta Petrologica Sinica*, *23*(11), 2981–2989. (in Chinese with English abstract)

Yan, Q. S., Shi, X. F., Wang, K. S., Bu, W. R., & Xiao, L. (2008). Major element, trace element, and Sr, Nd and Pb isotope studies of Cenozoic basalts from the South China Sea. *Science in China Series D: Earth Sciences*, *51*(4), 550–566.

Yan, Q. S., Shi, X. F., Wang, K. S., & Liu, X. M. (2008). LA-ICP-MS zircon U-Pb dating of granitic Rocks from the Nansha micro-block, South China Sea, and its geological Significance. *Acta Geologica Sinica*, *82*(8), 1057–1067.

Yan, Q. S., Shi, X. F., Yang, M. M., & Wang, K. S. (2008). Potassium-argon/argon-40- argon-39 geochronology of Cenozoic alkali basalts from the South China Sea. *Acta Oceanologica Sinica*, *27*(6), 115–123.

Yang, S. Y., & Fang, N. Q. (2015). Geochemical variation of volcanic rocks from the South China Sea and neighboring land: Implication for magmatic process and mantle structure. *Acta Oceanologica Sinica*, *34*(12), 112–124.

Yang, X. A., Chen, Y. C., Hou, K. J., Liu, S. B., & Liu, J. J. (2014). U–Pb zircon geochronology and geochemistry of Late Jurassic basalts in Maevatanana, Madagascar: Implications for the timing of separation of Madagascar from Africa. *Journal of African Earth Sciences*, *100*, 569–578.

Yang, Z., Zhang, G. X., Zhang, L., Wu, S. G., Zhu, Y. H., Qiang, K. S., & Yan, W. (2017). The spatial-temporal distribution of Miocene carbonate platform in the Xisha sea area and its model of hydrocarbon accumulation. *Acta Geologica Sinica*, *2017*, *91*(6), 1360–1373. (in Chinese with English abstract)

Yao, B. C., Wan, L., & Wu, N. Y. (2004). Cenozoic plate tectonic activities in the Great South China Sea area. *Geology in China*, *31*(2), 113–122. (in Chinese with English Abstract)

Yao, W. H., Li, Z. X., Li, W. X., Li, X. H., & Yang, J. H. (2014). From Rodinia to Gondwana land: Atale from detrital provenance analyses of the Cathaysia Block, South China. *American Journal of Science*, *314*(1), 278–313.

Yu, J. H., O'Reilly, S. Y., Wang, L., Griffin, W. L., Zhang, M., Wang, R. C., … Shu, L. S. (2008). Where was South China in the Rodinia supercontinent?: Evidence from U-Pb geochronology and Hf isotopes of detrital zircons. *Precambrian Research*, *164*(1–2), 1–15.

Yu, J. H., O'Reilly, S. Y., Wang, L., Griffin, W. L., Zhou, M. F., Zhang, M., & Shu, L. S. (2010). Components and episodic growth of Precambrian crust in the Cathaysia Block, South China: Evidence from U-Pb ages and Hf isotopes of zircons in Neoproterozoic sediments. *Precambrian Research*, *181*(1), 97–114.

Yu, J. H., O'Reilly, S. Y., Wang, L. J., Griffin, W. L., Jiang, S. Y., Wang, R. C., & Xu, X. S. (2007). Finding of ancient materials in Cathaysia and implication for the formation of Precambrian crust. *Chinese Science Bulletin*, *52*(1), 13–22.

Yu, J. H., O'Reilly, S. Y., Zhou, M. F., Griffin, W. L., & Wang, L. J. (2012). U-Pb geochronology and Hf–Nd isotopic geochemistry of the Badu Complex, Southeastern China: Implications for the Precambrian crustal evolution and paleogeography of the Cathaysia Block. *Precambrian Research*, *222–223*, 424–449.

Yu, J. H., Wang, L. J., O'Reilly, S. Y., Shu, L. S., & Sun, T. (2009). Paleoproterozoic basement beneath the southern Jiangxi Province: Evidence from U-Pb ages and Lu-Hf isotopes in zircons from the Doushui lamprophyre. *Chinese Science Bulletin*, *54*(9), 1555–1563.

Yu, L. F., Zhao, W. X., Chen, J. L., Guo, Q., & Wang, B. D. (2011). Compositional zone investigation of clinopyroxene phenocryst in the Cenozoic ultra-potassic rocks from the middle-southern Lhasa block. *Acta Petrologica Sinica*, *27*(12), 3666–3674. (in Chinese with English abstract)

Yuan, H. L., Gao, S., Dai, M. N., Zong, C. L., Günther, D., Fontaine, G. H., … DiWu, C. R. (2008). Simultaneous determinations of U–Pb age, Hf isotopes and trace element compositions of zircon by excimer laser ablation quadrupole and multiple collector ICP-MS. *Chemical Geology*, *247*(1–2), 100–118.

Zhang, Q. (2014). *Cenozoic Magmatism in the Northern Continental Margin of the South China Sea and its Implication for the Tectonic Evolution of the Rifted Margin*. Doctor Dissertation, Institute of Oceanology, Chinese Academy of Sciences, 1–119.

Zhang, J., Li, J. B., Ruan, A. G., Wu, Z. L., Yu, Z. T., Niu, X. W., & Ding, W. W. (2016). The velocity structure of a fossil spreading centre in the southwest sub-basin, South China Sea. *Geological Journal*, *51*(S1), 548–561.

Zhang, J., Li, J. Y., Liu, J. F., Liu, J. F., Qu, J. F., & Zhang, Y. P. (2013). LA-ICP-MS U-Pb ages of pillow lava basalts in southwestern Langshan, Inner Mongolia and their implication. *Geological Bulletin of China*, *32*(2/3), 287–296. (in Chinese with English abstract)

Zhang, J. W., Dai, C. G., Huang, Z. L., Luo, T. Y., Qian, Z. K., & Zhang, Y. (2015). Age and petrogenesis of Anisian magnesian alkali basalts and their genetic association with the Kafang stratiform Cu deposit in the Gejiu supergiant tin-polymetallic district, SW China. *Ore Geology Reviews*, *69*, 403–416.

Zhang, Q., Wu, S. G., & Dong, D. D. (2016). Cenozoic magmatism in the northern continental margin of the South China Sea: Evidence from seismic profiles. *Marine Geophysical Research*, *37*, 71–94.

Zhang, Q., Wu, S. G., Lv, F. L., Dong, D. D., Yan, Q. S., & Yang, Z. (2014). The seismic characteristics and the distribution of the igneous rocks in the northernwest slope of the South China Sea. *Geotectonica et Metallogenia*, *38*(4), 919–938. (in Chinese with English abstract)

Zhang, Y., Li, S. Z., Guo, L. L., Yu, S., Zhao, S. J., Somerville, I. D., … Mu, D. L. (2016). Origin of transform faults in back-arc basins: Examples from Western Pacific marginal seas. *Geological Journal*, *51*(S1), 490–512.

Zheng, J. P., Griffin, W. L., Li, L. S., O'Reilly, S. Y., Pearson, N. J., Tang, H. Y., … Su, Y. P. (2011). Highly evolved archean basement beneath the western cathaysia block, South China. *Geochimica et Cosmochimica Acta*, *75*(1), 242–255.

Zheng, J. P., Griffin, W. L., Tang, H., Zhang, Z., Su, Y., & Liu, G. (2008). Archean basement similar to the North China and Yangtze continents may be existed beneath the western Cathaysia. *Geological Journal of China Universities*, *14*(4), 549–557. (in Chinese with English abstract)

Zheng, Q. L., Li, S. Z., Suo, Y. H., Li, X. Y., Guo, L. L., Wang, P. C., … Somerville, I. D. (2016). Structures around the Tinjar-West Baram Line in northern Kalimantan and seafloor spreading in the proto-South China Sea. *Geological Journal*, *51*(S1), 513–523.

Zhou, X. M., Sun, T., Shen, W. Z., Shu, L. S., & Niu, Y. L. (2006). Petrogenesis of Mesozoic granitoids and volcanic rocks in South China: A response to tectonic evolution. *Episodes*, *29*(1), 26–33.

Zhu, J. J., Li, J., Sun, Z. X., & Li, S. Z. (2016). Crustal thinning and extension in the northwestern continental margin of the South China Sea. *Geological Journal*, *51*(S1), 286–303.

Zhu, W. L., Wang, Z. F., Mi, L. J., Du, X. B., Xie, X. N., Lu, X. C., … You, L. (2015). Sequence stratigraphic framework and reef growth unit of Well Xike-1 from Xisha Islands, South China Sea. *Earth Science—Journal of China University of Geosciences*, *40*(4), 678–687. (in Chinese with English abstract)

Zhu, W. L., Xie, X. N., Wang, Z. F., Zhang, D. J., Zhang, C. L., Cao, L. C., & Shao, L. (2017). New insights on the origin of the basement of the Xisha Uplift, South China Sea. *Science China Earth Sciences*, *60*, 1–8.

Zong, K. Q., Liu, Y. S., Gao, C. G., Hu, Z. H., Gao, S., & Gong, H. J. (2010). In situ U-Pb dating and trace element analysis of zircons in thin sections of eclogite: Refining constraints on the UHP metamorphism of the Sulu terrane, China. *Chemical Geology*, *269*(3–4), 237–251.

Zou, H. P. (1993). On the problem about the crust's, attribution of South China Sea basin-discussion from comparative study on basalts of sea mounts in South China Sea basin and the neighboring areas. *Geotectonica et Metallogenia*, *17*(4), 293–303. (in Chinese with English abstract)

SUPPORTING INFORMATION

Additional supporting information may be found online in the Supporting Information section at the end of the article.

How to cite this article: Zhang Y, Yu K, Qian H, et al. The basement and volcanic activities of the Xisha Islands: Evidence from the kilometre-scale drilling in the northwestern South China Sea. *Geological Journal*. 2019;1–13. https://doi.org/10.1002/gj.3416